Dynamical control of directional nonlinear scattering from metallic nanoantennas by three-dimensional focal polarization orientation*

WANG Xiang-hui (王湘晖)[1]**, **WANG Jian-xin** (王建鑫)[1], and **ZENG Ming** (曾明)[2]

1. Tianjin Key Laboratory of Micro-scale Optical Information Science and Technology, Institute of Modern Optics, Nankai University, Tianjin 300350, China

2. School of Electrical Engineering and Automation, Tianjin University, Tianjin 300072, China

(Received 2 January 2020; Revised 6 April 2020)

We demonstrate that the directionality of far-field second harmonic (SH) emission generated from individual gold nanosphere can be flexibly engineered by manipulating three-dimensional (3D) focal polarization orientation of the excitation field, which is explained by the coherent interference between SH dipolar and quadrupolar emission modes. The SH dipolar emission mode is independent of the polarization direction of the fundamental field whereas the evolution of the focal polarization orientation can dramatically modify the quadrupolar emission pattern. Therefore, the resultant SH emission pattern has a polarization-dependent behavior and side scattering almost perpendicular to the propagation direction of the incident light can be observed under a specific condition. Our findings provide a novel degree of freedom for all-optical control of directional nonlinear scattering from single nanoantenna, thereby opening new possibilities for future potential applications.

Document code: A **Article ID:** 1673-1905(2021)02-0065-5

DOI https://doi.org/10.1007/s11801-021-0001-1

Optical nanoantennas have attracted a lot of interest due to their capability to manipulate light-matter interactions at the nanoscale[1]. Tailoring the nanoantenna's far-field radiation in a preferential direction plays an important role in many applications such as photodetection[2], sensing[3], wireless communications[4], quantum manipulation[5], integrated optics[6]. Directional control of linear optical responses from plasmonic[5-7], dielectric[8], and hybrid nanoantennas[9,10] have been extensively studied. In parallel to the investigation of linear scattering of nanoantennas, interest in their nonlinear counterparts, and more specifically second harmonic generation (SHG), is growing rapidly[11-16]. For example, a compact nonlinear Yagi-Uda nanoantenna[11] has been proposed to realize SH radiation bent at 90° with respect to the incident light direction. By rotating the polarization of the incident light, forward and backward switching of SHG emission directionality is obtained[14]. By adjusting the relative position of the nanoantenna in the fundamental field, directivity change for SH emission could be observed[15]. However, there is little research about simultaneously controlling radial and azimuthal angles of SHG emission directionality.

Light polarization state play an important role in the light-matter interaction[5,17,18]. For conventional polarized beams, such as linear and circular polarization, light polarization direction is always confined to the plane perpendicular to the propagation direction. When a radially polarized beam is tightly focused, a longitudinal polarization state can be obtained in the focal volume[19]. Some dynamic methods have been proposed to generate arbitrary three-dimensional (3D) polarization orientation in the focus[20-22]. It has been demonstrated that spatial orientation detection[21] or orientation unlimited polarization encryption[22] of nanorods can been realized by using those kinds of focused fields.

In this letter, we present angular control of directional nonlinear scattering from single gold nanosphere by 3D polarization orientation. 3D focal polarization orientation is realized by coherent superposition of a linearly and a radially polarized beam focused by a high numerical aperture (NA) objective. The electric fields in the region located by the gold nanosphere are locally linearly polarized and can be arbitrarily tuned in 3D spatial directions. Far-field SH responses from the gold nanosphere for different focal polarization orientation are investigated. It is shown that due to the fact that dipolar and quadrupolar SH emission modes exhibit different polarization

* This work has been supported by the Key Program of the Natural Science Foundation of Tianjin (No.19JCZDJC32700), and the Science and Technology Support Program of Tianjin (No.17YFZCSY00740).

** E-mail: wangxianghui@nankai.edu.cn

dependences, the coherent interference between those two modes can be harnessed for controlling the directionality of far-field nonlinear emission from metallic nanoantennas through the 3D manipulation of the focal polarization orientation.

See Fig.1, as a consequence of coherent superposition of linearly and radially polarized beams focused by an infinity-corrected objective, the three components of the superposed electric field at a given point $\boldsymbol{r}_p$ in the focal region take the form

$$\begin{aligned} E_{exc}^{x} &= w_1 E_L^{x} + \mathrm{i} w_2 E_R^{x}, \\ E_{exc}^{y} &= w_1 E_L^{y} + \mathrm{i} w_2 E_R^{y}, \\ E_{exc}^{z} &= w_1 E_L^{z} + \mathrm{i} w_2 E_R^{z}, \end{aligned} \tag{1}$$

where the superscripts L and R refer to linearly and radially polarized beams, respectively. w_1 and w_2 are the weighting factors of focused linearly and radially beams, respectively, ranging from 0 to 1. When w_1=1 and w_2=0, the incident beam is x-linearly polarized. The relative magnitudes of those two parameters are adjusted by the density filter in Fig.1. In the framework of the vectorial diffraction theory[19,23], the components E_R^x, E_R^y, and E_R^z of the focused radially-polarized beam follow the notation of Ref.[24] and the components E_L^x, E_L^y, E_L^z of the focused linearly-polarized beam can be expressed as

$$\begin{aligned} E_L^{x} &= -\mathrm{i}\cos(2\varphi)[I_0 + I_2\cos(2\phi_p)] - \\ &\quad \mathrm{i}\sin(2\varphi) I_2 \sin(2\phi_p), \\ E_L^{y} &= -\mathrm{i}\cos(2\varphi) I_2 \sin(2\phi_p) - \\ &\quad \mathrm{i}\sin(2\varphi)[I_0 - I_2\cos(2\phi_p)], \\ E_L^{z} &= -2\cos(2\varphi) I_1 \cos(\phi_p) - \\ &\quad 2\sin(2\varphi) I_1 \sin(\phi_p), \end{aligned} \tag{2}$$

where ϕ_p is the azimuthal angle of the point $\boldsymbol{r}_p$ and φ is the polarization direction of the incident linearly polarized beam with respect to the optical axis of the half-wave plate. The values of φ corresponding to an x- or y-linearly polarized beam are 0° and 45°, respectively. The integrals I_n take the forms in Ref.[24].

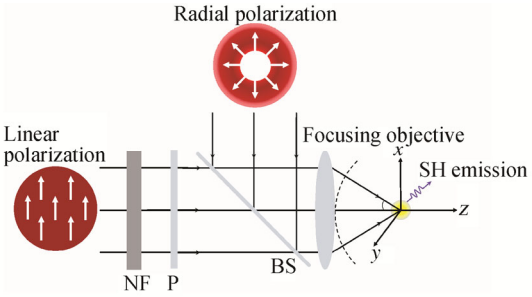

NF: appropriate neutral density filter; P: half-wave plate; BS: beam splitter

Fig.1 Illustration of the scheme for generating 3D linear polarization in the focal region

In the practical experiments, the relative magnitudes of w_1 and w_2 are manipulated by properly adjusting the intensity of the incident linearly polarized beam. Then, the focal polarization can be tuned between transverse and longitudinal polarization states with respect to the optical axis (see Fig.1 in Ref.[21]). Furthermore, 3D polarization orientation in the focal plane can be finally realized by tuning the azimuthal angle φ of the linearly polarized beam, which is usually achieved by the rotation of the half-wave plate.

A gold nanosphere with a diameter of 100 nm is choosen as single-nanoparticle antenna. For metallic nanoantennas located at the focal region, the fundamental excitation field can be calculated using the scattered-field formalism for finite-difference time-domain (FDTD) numerical solution[25] since the incident field can be obtained analytically. Simulation of SH response from metallic nanoantennas can be calculated by using the Green's function approach[24]. In addition, only the component $\chi_{s,\perp\perp\perp}$ (where $\perp$ refers to the direction normal to the local surface of metallic nanoantennas) of the surface second-order susceptibility tensor is taken into account since this element generally dominates the surface SH response of metallic nanoparticles under the electric dipolar approximation[26,27].

The fundamental wavelength is 780 nm and the incident fundamental beam is focused by a dry objective with NA=0.9. The medium surrounding nanoparticles is assumed to be air. The mesh grid is set to 2.5 nm in all directions. The time step Δt is smaller than the Courant time step t_c and takes the value of $0.9t_c$. A convolutional perfect matched layer is set at all surrounding boundaries.

After focused by a high NA objective, the field vector in the focal region is likely to be elliptically polarized[23] due to the emergence of new field components induced by the refraction effect of the focusing objective. The polarization state can be obtained in terms of the real and imaginary parts of the field vector[23]. When φ=0, Fig.2 illustrates distributions for the ratio of the short and long semi-axes of the polarization ellipse in the focal plane for different values of w_1 and w_2. Figs.2(a) and (d) correspond to x-linear and radial polarization illuminations, respectively. The black circle denotes the location of the gold nanosphere. For w_1=1 and w_2=0, i.e., the incident beam is x-linearly polarized, the distribution in Fig.2(a) agrees well with the result in Fig.2(b) in Ref.[23]. It can be found that the local polarization of the focal field exhibits obvious position dependence. In the focus, the value of the ratio for the two semi-axes of the polarization ellipse is zero, which indicates that the focal polarization is linearly polarized. In the region away from the focus, the value of the ratio increases, the polarization state is progressively changed from linear to elliptical. When it approaches 1, circular polarization occurs. However, it should be also noted that in the region located by the gold nanosphere, the value of the ratio for the two semi-axes of the polarization ellipse doesn't be-

yond 0.1. Therefore, the fields in the vicinity of the focus are locally linearly polarized because the x component is dominant under x-linear polarization illumination[23]. As the relative magnitude of w_2 increases, the electric fields around the focus always maintain dominantly linearly polarized.

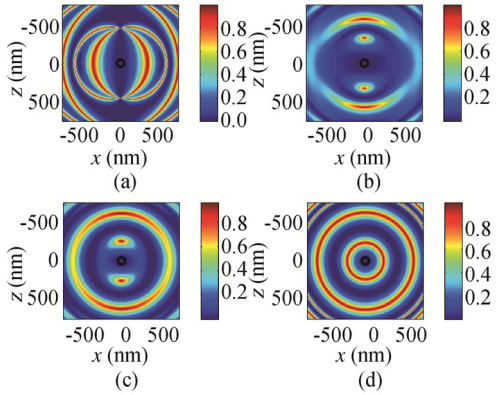

Fig.2 When φ=0, distributions for the ratio of the two semi-axes of the polarization ellipse in the focal plane for (a) w_1=1, w_2=0, (b) w_1=0.866, w_2=0.5, (c) w_1=0.5, w_2=0.866, (d) w_1=0, w_2=1, respectively

When φ=0, distributions for intensity of the superposed field and polarization orientation in the focal plane for different values of w_1 and w_2 are presented by Fig.3. The intensities have been normalized to the maximum in the focus. The pink arrow denotes the polarization orientation. When w_1=1 and w_2=0, the field in the vicinity of the focus is x-linearly polarized because the x component is dominant under x-linear polarization illumination. When w_1=0.866 and w_2=0.5, the polarization orientation rotates away from the z axis and the angle between the polarization direction and the z axis is about 60°. This angle decreases to be 30° when w_1=0.5 and w_2=0.866. For the case of radial polarization illumination (see the result in Fig.3(d)), the polarization direction is oriented to the z axis, which is attributed to the strong longitudinal component in the focus[19]. Briefly, for those four kinds of cases illustrated in Fig.3, the corresponding axial angles (defined as Θ) of the focal polarization orientation with respect to the z axis are 90°, 60°, 30° and 0°, respectively.

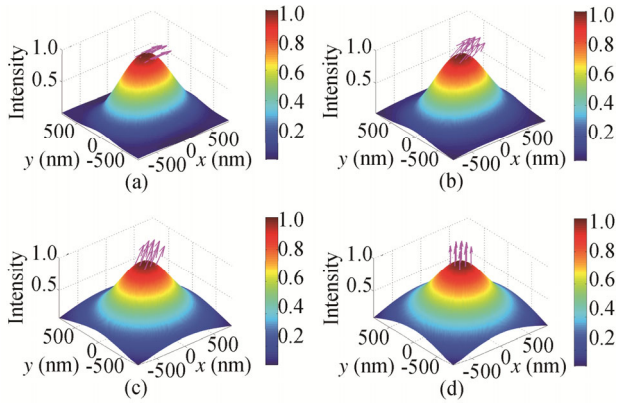

Fig.3 When φ=0, 3D field view of normalized intensity and polarization orientation distributions in the focal plane for (a) w_1=1, w_2=0, (b) w_1=0.866, w_2=0.5, (c) w_1=0.5, w_2=0.866, (d) w_1=0, w_2=1, respectively (Only the polarization orientations in the region located by the gold nanosphere are presented by the pink arrows.)

The azimuthal angle Φ of the focal polarization relative to the x axis can be tuned by rotating the half-wave plate in Fig.1 and has a dependence of Φ=2φ. Here, φ is the polarization direction of the linearly-polarized incident field. Fig.4 illustrates the focal polarization orientation for different values of Φ when Θ=60°. The inset of Fig.4 gives the projection of the focal polarization orientation in the xy plane, which rotates anticlockwise.

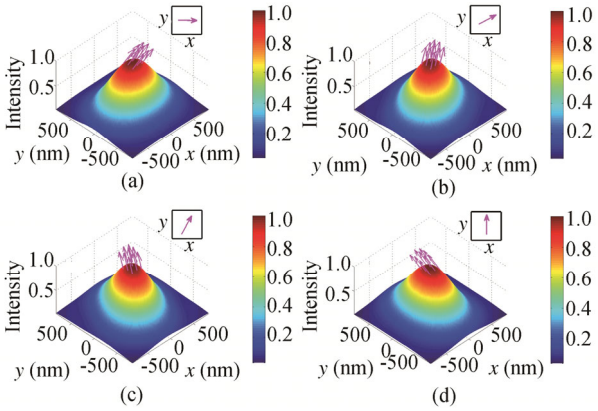

Fig.4 When Θ=60°, 3D field view of normalized intensity and polarization orientation distributions in the focal plane for (a) Φ=0°, (b) Φ=30°, (c) Φ=60°, (d) Φ=90°, respectively

Fig.5 gives 3D far-field SH angular radiation diagrams of single gold nanosphere with 100 nm diameter for different values of Θ. The corresponding cuts in the xz plane are presented by the second column of Fig.5. Each pattern has already been normalized to its own maximum. From the result in Figs.5(a) and (b), for x-linear polarization, SH angular emission presents four lobes pattern with two strong lobes forward-propagating in an off-axis direction and there are no SH signal in the exact forward and backward directions due to the selection rule as the consequence of the rotational symmetry of the particle shape around the longitudinal direction[28]. The radial angle of SH radiation directionality relative to the z axis is about 45°. However, according to Figs.5(c), (d), (e) and (f), as the focal polarization orientation progressively rotates away from the x axis, the SH response presents asymmetrical scattering pattern and the whole emission pattern rotates clockwise. Some lobes obviously shrink and even completely vanishes (see Fig.5(f)). In addition, quite surprisingly, it is found that the SH intensity is not strictly zero in the exact forward and backward directions, which is not the same as the previous expectation

for nanoparticles with a centrosymmetric shape and can be attributed to the fact that the exciting fundamental field becomes asymmetrical about the propagation direction. As shown in Figs.5(g) and (h), for radial polarization, strong backward emission is observed while there is only negligible SH signal in the forward direction. From the evolution of the SH response in Fig.5, it can be concluded that directional nonlinear scattering from the gold nanosphere can be dynamically engineered by the manipulation of the focal polarization orientation.

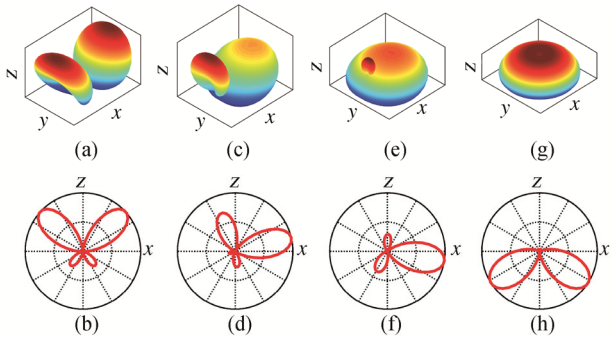

Fig.5 When φ=0, far-field SH angular radiation patterns for (a, b) Θ=90°, (c, d) Θ=60°, (e, f) Θ=30°, (g, h) Θ=0°, respectively

In order to elucidate the above phenomena in Fig.5, it is very useful to investigate the multipolar properties about SHG from a nanosphere of centrosymmetric material. In a multipole expansion, the SH radiation of spherical nanoparticles can be presented in terms of an effective dipole moment composed of two leading-order moments, the dipolar and quadrupolar contributions[29], which has be experimentally evidenced by various polarization-resolved measurements[30]. A careful examination shows that the dipolar moment is independent of the polarization direction of the exciting fundamental field and is always oriented parallel to the propagation direction of the incident fundamental beam while the orientation of the quadrupolar moment could change accordingly with the polarization direction for the pump beam. The first row of Fig.6 presents the pure SH emission from a dipolar moment orienting along the propagation direction while the second row gives the pure quadrupolar emission when the relative angle between the orientation of the quadrupolar moment and the z axis is 90°, 60°, 30°, 0°, respectively. The emissions from coherent interaction between the dipolar and quadrupolar moments are illustrated by the third row of Fig.6. The strength ratio of the dipolar and quadrupolar moments is 0.65 and the phase difference between those two moments is $\pi/2$. A comparison of Figs.5 and 6 distinctly demonstrates that the presence of the dipolar and quadrupolar contributions and their different dependences on the polarization direction of the fundamental excitation field result in the possibility for dynamical manipulation of directional nonlinear scattering from the gold nanosphere by adjusting the focal polarization orientation. For the gold nanosphere with the diameter of 100 nm, although an octupolar response in the harmonic field component parallel to the scattering plane has been observed[31], the interference between the dipolar and quadrupolar contributions is enough to be used to qualitatively explained the phenomena in Fig.5.

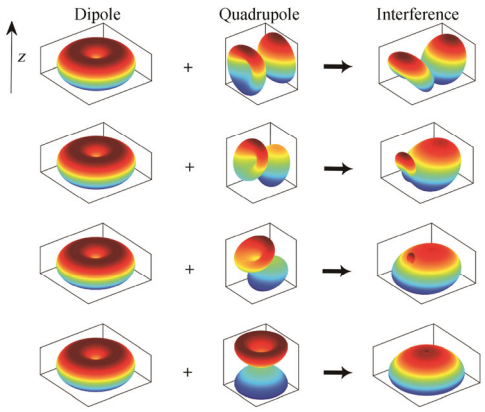

Fig.6 Far-field SH angular radiation patterns from the dipolar moment (first row), quadrupolar moment with different orientations (second row) and multipolar interaction between the dipolar and quadrupolar modes (third row), respectively

If the relative magnitude between linear and radial polarizations, that is, the ratio of w_1 and w_2, is fixed, while the polarization direction of the linearly-polarized incident light is adjusted by the half-wave plate in Fig.1, the azimuthal angle Φ of the focal polarization could be manipulated (see Fig.4). For Θ=60°, far-field SH angular radiation patterns of single gold nanosphere for different values of Φ are presented by Fig.7. The results show that the whole SH emission pattern is unchanged while its orientation rotates with respect to the x axis, which indicates that the azimuthal angle of directional SH radiation is tunable. The results for other values of Θ are identical and not presented for the sake of simpilicity.

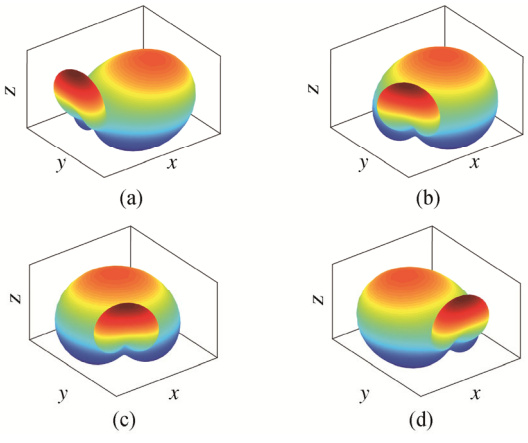

Fig.7 When Θ=60°, far-field SH angular radiation patterns for (a) Φ=0°, (b) Φ=30°, (c) Φ=60°, (d) Φ=90°, respectively

It has been demonstrated that the relative phase between dipolar and quadrupolar emission modes is related to the excitation wavelength, which results in the variation of SH radiation pattern[32]. However, for a specific incident wavelength, the dependences of dipolar and quadrupolar emission modes on the focal polarization orientation remain unchanged. Therefore, it is still valid to control the directionality of SH radiation pattern by the focal polarization orientation.

In summary, we have numerically demonstrated the possibility to dynamically control the axial and azimuthal directions of directional nonlinear scattering generated from single metallic nanoparticle by the manipulation of 3D focal polarization orientation of the fundamental beam. The evolution of the far-field SH emission with the focal polarization orientation is explained by multipolar interference between the dipolar and quadrupolar contributions, which is attributed to their different dependences on the focal polarization orientation of the excitation field. Our investigations are beneficial for a better understanding of the fundamental light-matter interactions in metal nanoparticles and provide the guideline for the manipulation of nonlinear optical response of metal particles through optical beam engineering, thereby opening possibilities for a wide range of practical applications such as imaging probes to collect signals, short wavelength nanolasers and all-optical switchers for waveguides.

References

[1] L. Novotny and N. van Hulst, Nature Photonics **5**, 83 (2011).

[2] M.W. Knight, H. Sobhani, P. Nordlander and N. J Halas, Science **332**, 702 (2011).

[3] J. N. Anker, W. P. Hall, O. Lyandres, N. C. Shah, J. Zhao and R. P. Van Duyne, Nature Materials **7**, 442 (2008).

[4] M. Elsaid, K. R. Mahmoud, M. F. O. Hameed, S. S. A. Obayya and M. Hussein, Journal of the Optical Society of America B **37**, 1183 (2020).

[5] M. Neugebauer, T. Bauer, P. Banzer and G. Leuchs, Nano Letters **14**, 2546 (2014).

[6] J. Li, N. Verellen, D. Vercruysse, T. Bearda, L. Lagae and P. Van Dorpe, Nano Letters **16**, 4396 (2016).

[7] P. R. Wiecha, C. Majorel, C. Girrard, A. Cuche, V. Paillard, O. L. Muskens and A. Arbouet, Optics Express **27**, 29069 (2019).

[8] Y. H. Fu, A. I. Kuznetsov, A. E. Miroshnichenko, Y. F. Yu and B. Luk'yanchuk, Nature Communications **4**, 1527 (2013).

[9] A. Devilez, B. Stout and N. Bonod, ACS Nano **4**, 3390 (2010).

[10] E. Rusak, I. Staude, M. Decker, J. Sautter, A. E. Miroshnichenko, D. A. Powell, D. N. Neshev and Y. S. Kivshar, Applied Physics Letters **105**, 221109 (2014).

[11] X. Y. Z. Xiong, L. J. Jiang, W. E. I. Sha, Y. H. Lo and W. C. Chew, Scientific Reports **6**, 18872 (2016).

[12] L. Carletti, A. Locatelli, D. Neshev and C. D. Angelis, ACS Photonics **3**, 1500 (2016).

[13] X. Y. Z. Xiong, L. J. Jiang, W. E. I. Sha, Y. H. Lo, M. Fang, W. C. Chew and W. C. H. Choy, Physical Review A **94**, 053825 (2016).

[14] L. Xu, G. Saerens, M. Timofeeva, D. A. Smirnova, I. Volkovskaya, M. Lysevych, R. Camacho-Morales, M. Cai, K. Z. Kamali, L. Huang, F. Karouta, H. H. Tan, C. Jagadish, A. E. Miroshnichenko, R. Grange, D. N. Neshev and M. Rahmani, ACS Nano **14**, 1379 (2020).

[15] K. Yoo, S. F. Becker, M. Silies, S. Yu, C. Lienau and N. Park, Optics Express **27**, 18246 (2019).

[16] D. K. Sharma, S. K. Chaubey, A. B. Vasista, J. J. Karumancheril, R. P. N. Tripathi, A. Bouhelier and G. V. P. Kumar, Applied Optics **57**, 5914 (2018).

[17] J. Lin, J. P. B. Mueller, Q. Wang, G. Yuan, N. Antoniou, X.-C. Yuan and F. Capasso, Science **340**, 331 (2013).

[18] M. Neugebauer, P. Woźniak, A. Bag, G. Leuchs and P. Banzer, Nature Communications **7**, 11286 (2016).

[19] K. S. Youngworth and T. G. Brown, Optics Express **7**, 77 (2000).

[20] A. F. Abouraddy and K. C. Toussaint Jr, Physical Review Letters **96**, 153901 (2006).

[21] P. Olk, T. Härtling, R. Kullock and L. M. Eng, Applied Optics **49**, 4479 (2010).

[22] X. Li, T.-H. Lan, C.-H. Tien and M. Gu, Nature Communications **3**, 998 (2012).

[23] B. Richards and E. Wolf, Proceedings of the Royal Society of London. Series A. Sciences **253**, 358 (1959).

[24] J. Sun, X.Wang, S. Chang, M. Zeng, S. Shen and N. Zhang, Optics Express **24**, 7477 (2016).

[25] W. A. Challener, I. K. Sendur and C. Peng, Optics Express **11**, 3160 (2003).

[26] G. Bachelier, J. Butet, I. Russier-Antoine, C. Jonin, E. Benichou and P.-F. Brevet, Physical Review B **82**, 235403 (2010).

[27] J. Butet, K. Thyagarajan and O. J. F Martin, Nano Letters **13**, 1787 (2013).

[28] M. Finazzi, P. Biagioni, M. Celebrano and L. Duò, Physical Review B **76**, 125414 (2007).

[29] J. I. Dadap, J. Shan and T. F. Heinz, Journal of the Optical Society of America B **21**, 1328 (2004).

[30] J. Nappa, G. Revillod, I. Russier-Antoine, E. Benichou, C. Jonin and P. F. Brevet, Physical Review B **71**, 165407 (2005).

[31] J. Butet, G. Bachelier, I. Russier-Antoine, C. Jonin, E. Benichou and P.-F. Brevet, Physical Review Letters **105**, 077401 (2010).

[32] J. Butet, T. V. Raziman, K.-Y. Yang, G. D. Bernasconi and O. J. F. Martin, Optics Express **24**, 17138 (2016).